

## Equation of State of Magnesite for the Conditions of the Earth's Lower Mantle

P. I. Dorogokupets

*Institute of the Earth's Crust, Siberian Division, Russian Academy of Sciences,  
ul. Lermontova 128, Irkutsk, 664033 Russia*

*e-mail: dor@crust.irk.ru*

Received December 29, 2005

**Abstract**—A semiempirical equation of state was derived for magnesite under the thermodynamic conditions of the Earth's mantle. Within experimental uncertainties, it is consistent with thermochemical, ultrasonic, X-ray, and shock-wave data at temperatures from 15 K to the melting point and pressures of up to 100–130 GPa. The following values were recommended for the isothermal bulk modulus and its pressure derivative:  $K_T = 111.71$  GPa and  $K' = 4.08$ . Thermodynamic analysis showed that magnesite does not decompose to periclase and  $\text{CO}_2$  under the thermodynamic conditions of the Earth's lower mantle and outer core.

**DOI:** 10.1134/S0016702907060043

Recent experimental studies [1, 2] have shown that magnesite ( $\text{MgCO}_3$ ) is stable and retains its structure to a pressure of at least  $\sim 110$  GPa at temperatures of 2000–3000 K. At a pressure of  $\sim 115$  GPa, magnesite converts to a new form, which was referred to as magnesite II by Isshiki et al. [2]. First principles calculations [3] showed that magnesite transforms into a pyroxene structure at a pressure of 113 GPa and into a  $\text{CaTiO}_3$ -type structure above 200 GPa, which is in agreement with direct experimental measurements. Consequently, magnesite is stable under the  $P$ - $T$  parameters of the Earth's upper and lower mantle and outer core. Phase relations of magnesite with silicates at high temperatures and pressures are of considerable interest for the assessment of the role of carbon in the Earth's interiors and have been a subject of extensive experimental research (for instance, see the review of Liu [4]). Of equal importance in the investigation of carbonate–silicate phase relations is the thermodynamic analysis of physicochemical processes in the Earth's interiors [5, 6], the reliability of which is primarily controlled by the quality of thermodynamic information. It is no wonder, therefore, that a number of models has been proposed during the past decades for the equation of state of minerals that can be used to solve this problem [7–16]. They concern mainly silicates and oxides. The thermodynamic properties of carbonates are available, for instance, in the database of Holland and Powell [17], but they are not appropriate for the thermodynamic analysis of phase relations under the conditions of the Earth's upper and lower mantle. Because of this, the goal of the present study was to comprehensively evaluate experimental and theoretical data for magnesite, derive its equation of state, and analyze magnesite

stability under the thermodynamic conditions of the Earth's lower mantle.

The equation of state of magnesite was derived on the basis of the modified formalism proposed in [12, 15, 18]. The Helmholtz free energy is written as a sum of several contributions, one of which depends on volume only and others, on temperature and volume:

$$F = U_0 + E(V) + F_{\text{qh}}(V, T) + F_{\text{anh}}(V, T), \quad (1)$$

where  $U_0$  is the reference energy, which is introduced to obtain reference  $\Delta H_{f, 298}$  values under standard conditions;  $E(V)$  is the potential (cold) part of the free energy on the reference isotherm which depends on volume ( $V$ ) only;  $F_{\text{qh}}(V, T)$  is the quasiharmonic part of the Helmholtz free energy, which is a function of volume and temperature; and  $F_{\text{anh}}(V, T)$  is the contribution of intrinsic anharmonicity.

The cold energy is expressed as [19]

$$E(V) = 9K_0V_0\eta^{-2}[1 - [1 - \eta(1 - y)]\exp[(1 - y)\eta]], \quad (2)$$

where  $y = x^{1/3} = (V/V_0)^{1/3}$  and  $\eta = 1.5(K' - 1)$ .

The quasiharmonic part of the Helmholtz free energy is approximated as

$$F_{\text{qh}} = \sum_1^i m_{\text{Bi}}R \left[ \frac{(d_i - 1)}{2d_i} \Theta_{\text{Bi}} - T \ln(1 + b_i) \right] + \sum_1^j m_{\text{Ej}}R \left[ \frac{\Theta_{\text{Ej}}}{2} + T \ln \left( 1 - \exp \frac{-\Theta_{\text{Ej}}}{T} \right) \right], \quad (3)$$

where  $\Theta_{\text{Bi}}$  and  $\Theta_{\text{Ej}}$  are the characteristic temperatures depending on volume, which is usually expressed in a dimensionless form as  $x = V/V_0$  ( $V_0$  is the volume under

**Table 1.** Parameters of the equations of state of magnesite and periclase

Parameter	MgCO <sub>3</sub>	MgO
$U_0$ , J/mol	-1 130 999	-609 687
$V_0$ , cm <sup>3</sup>	28.018	11.248
$K_0$ , GPa	111.71	160.31
$K'$	4.08	4.18
$\Theta_{B1}$ , K	339.3	447.3
$d_{B1}$	6.479	11.243
$m_{B1}$	3.350	1.429
$\Theta_{B2}$ , K	828.8	384.0
$d_{B2}$	12.635	3.593
$m_{B2}$	3.914	0.276
$\Theta_{E1}$ , K	1677.6	703.8
$m_{E1}$	3.914	2.570
$\Theta_{E2}$ , K	384.1	446.0
$m_{E2}$	4.125	1.725
$\gamma_0$	1.048	1.528
$\gamma_\infty$	0.757	1.111
$\beta$	-	4.509
$a$ , K <sup>-1</sup> *E6	-20.5	13.56
$m$	1.5	5.23

standard conditions);  $d_i$  is the exponential parameter controlling the behavior of the heat capacity near 0 K;  $b = 1/[\exp(g) - 1]$ ,  $g = d \ln[1 + \Theta_B/(Td_i)]$ ; and  $m_{B_i}$  and  $m_{E_j}$  are the degrees of freedom, the sum of which must be  $3n$ , where  $n$  is the number of atoms in the unit cell.

The volume dependence of characteristic temperatures was expressed after [20] as

$$\Theta = \Theta_0 x^{\gamma_\infty} \exp\left[\frac{\gamma_0 - \gamma_\infty}{\beta}(1 - x^\beta)\right], \quad (4)$$

where  $\gamma_0$ ,  $\gamma_\infty$ , and  $\beta$  are adjusted parameters. It was assumed that the  $\gamma_\infty$  and  $\beta$  values of magnesite are linked by the equation  $\beta = \gamma_0/(\gamma_0 - \gamma_\infty)$  [20]. Equation (4) yields

$$\gamma = -\frac{\partial \ln \Theta}{\partial \ln V} = \gamma_\infty + (\gamma_0 - \gamma_\infty)x^\beta,$$

$$q = \frac{\partial \ln \gamma}{\partial \ln V} = \beta x^\beta \frac{\gamma_0 - \gamma_\infty}{\gamma}.$$

The contribution of anharmonicity is expressed in the form [21] (other models were discussed in [22, 23])

$$F_{\text{anh}} = 3nR \frac{ax^m}{6} \times \left[ \left( \frac{1}{2} \Theta + \frac{\Theta}{e^{\Theta/T} - 1} \right)^2 + 2 \left( \frac{\Theta}{T} \right)^2 \frac{e^{\Theta/T}}{(e^{\Theta/T} - 1)^2} \times T^2 \right]. \quad (5)$$

Pressure on the shock-wave adiabat was calculated using the equation [18]

$$P_H = \frac{P(x) - \frac{\gamma}{V}[E(x) - E_0]}{1 - \frac{\gamma(1-x)}{2x}}. \quad (6)$$

Then, taking into account these analytical expressions, all the desired thermodynamic functions can be obtained by differentiating Eq. (1) with respect to temperature at constant volume and with respect to volume at constant temperature: entropy  $S = -(\partial F/\partial T)_V$ , internal energy  $E = F + TS$ , constant volume heat capacity  $C_V = (\partial E/\partial T)_V$ , pressure  $P = -(\partial F/\partial V)_T$ , isothermal bulk modulus  $K_T = -V(\partial P/\partial V)_T$ , and pressure slope at constant volume  $(\partial P/\partial T)_V = \alpha K_T$ , where  $\alpha = 1/V(\partial V/\partial T)_P$ . Heat capacity at constant pressure is determined from  $C_P = C_V + \alpha^2 TVK_T$ , adiabatic bulk modulus is  $K_S = K_T + VT(\alpha K_T)^2/C_V$ , enthalpy is  $H = E + PV$ , and the Gibbs free energy is  $G = F + PV$ . Thus, all the necessary thermodynamic functions can be determined as functions of  $T$  and  $P$  or  $T$  and  $V$ .

It should be noted that, during the practical implementation of the equation of state, the Helmholtz free energy is written as  $F = U_0 + E(V) + F(V, T) - F(V, T_0)$ , and the obtained fitted parameters of the equation of state correspond, therefore, to the reference conditions  $T_0 = 298.15$  K and  $P_0 = 1$  bar. Furthermore, it should be kept in mind that Eqs. (1)–(6) are written as functions of temperature and volume, and the calculation of thermodynamic functions under given  $T$  and  $P$  must involve a preliminary determination of volume from these equations.

The results of simultaneous treatment of the experimental measurements of the heat capacity [24, 25] and thermal expansion of magnesite [26], ultrasonic [27, 28],  $V$ - $P$  [29–33],  $V$ - $P$ - $T$  [34], and shock data [35] are illustrated below in diagrams and the adjusted parameters are given in Table 1. Figures 1 and 2 show the deviation of calculated heat capacity values from experimental data at low temperatures, heat capacity at constant pressure and constant volume, thermal expansion coefficient, and adiabatic and isothermal bulk moduli as functions of temperature at zero pressure, which are compared with the available experimental and computational data. Also shown are the isobaric heat capacity and thermal expansion coefficient of magnesite at pressures of 3 and 100 GPa.

The low-temperature heat capacity is in good agreement with the measurements of [24] (Fig. 1a), and the calculated standard entropy of magnesite,  $S_{298} = 65.07$  J/mol K, coincides with the data of [24, 25]. The high-temperature isobaric heat capacity is in good agreement with the values given in the handbook of Robie et al. [25] (Fig. 1b) and the value calculated by Matas et al. [36], who used an equation of state based on the analysis of the IR and Raman spectra of magne-

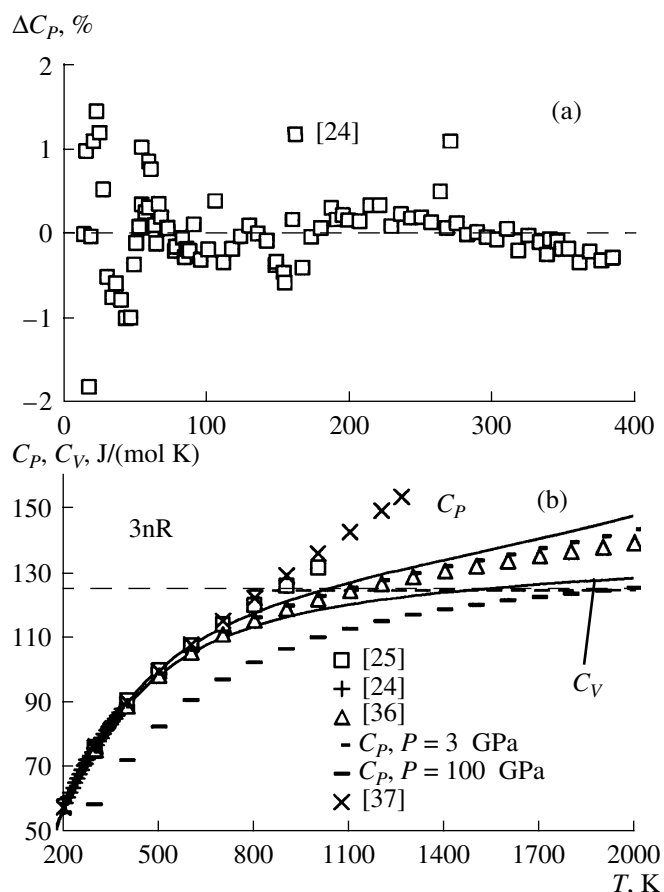


**Fig. 1.** (a) Deviation of the calculated heat capacity of magnesite from experimental data at low temperatures, ( $\Delta C_p = (C_{p\text{exp}} - C_{p\text{cal}})/C_{p\text{exp}} \times 100$ ) and (b) heat capacities at constant pressure and constant volume at pressures of 1 bar, 3 GPa, and 100 GPa.

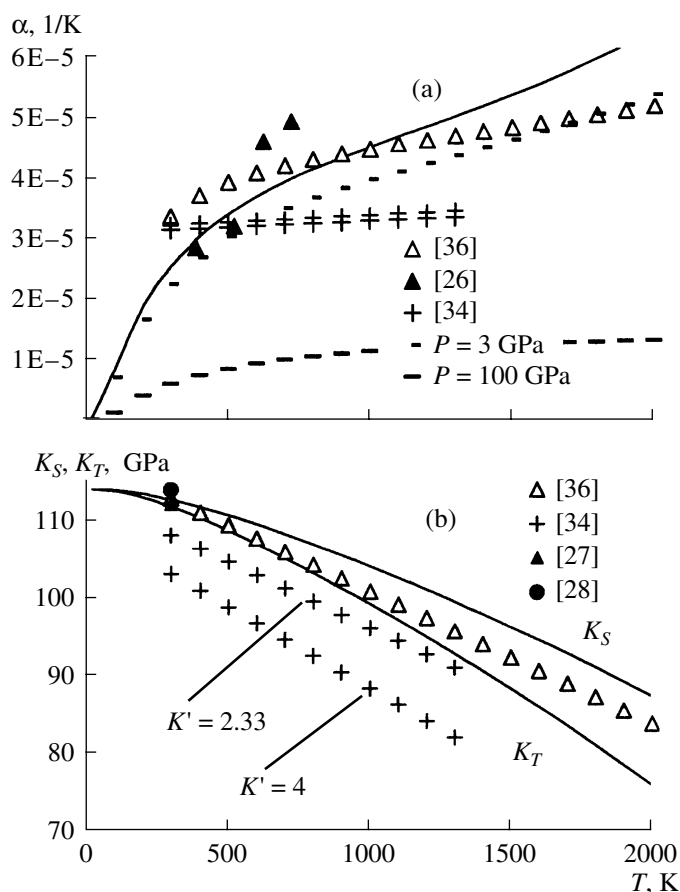


**Fig. 2.** (a) Thermal expansion coefficients at pressures of 1 bar, 3 GPa, and 100 GPa. (b) Adiabatic and isothermal bulk moduli at atmospheric pressure compared with the available experimental and computational data.

site. Noteworthy is the very high isobaric heat capacity of magnesite at temperatures higher than 1000 K according to the handbook of [37]. Such a considerable increase in heat capacity can only be provided by a very large value of the anharmonicity parameter, which is not supported by experiments [36]. In contrast to metals [15], the comprehensive estimation of the anharmonicity parameters  $a$  and  $m$  of magnesite is hampered by the scarcity of experimental measurements (e.g., thermal expansion coefficient at low temperatures and adiabatic bulk modulus as a function of temperature); therefore, we accepted  $m = 1.5$  after [36]. The isobaric heat capacity of magnesite obtained here is slightly higher than high-temperature  $C_p$  calculated by Matas et al. [36] but significantly lower than the handbook values [25, 37]. Our calculations for  $\alpha(T)$  and  $K_T(T)$  are in adequate agreement with the results of [36] (Fig. 2), and the difference in slope is related to the different values of the anharmonicity and Gruneisen parameters.

Zhang et al. [34] reported the results of  $V$ - $P$ - $T$  measurements for magnesite up to a pressure of 8.6 GPa

and a temperature of 1285 K. These authors fitted their data to the high-temperature Birch–Murnaghan equation in two approximations: (1) the parameter  $K' = dK_T/dP$  was fixed at  $K' = 4$  and (2)  $K'$  was adjusted to 2.33. As a result, they obtained almost identical  $\alpha(T)$  dependencies and contradictory results for the isothermal bulk modulus (Fig. 2). The second variant with the lower  $K'$  value is more consistent with ultrasonic measurements [27, 28]. This demonstrates that the processing of  $V$ - $P$ - $T$  data only without invoking even the simplest models of the equation of state (for instance, the Mie–Gruneisen–Debye model) cannot be successful in terms of the choice of a physically justified variant.

The volume–pressure ( $V$ - $P$ ) relations of magnesite were studied up to a pressure of 110 GPa at room temperature [2, 30–33, 38]. Based on thermodynamic considerations, the measurements of [30, 38] plotting above the shock adiabat of [35] in the  $P$ - $x$  diagram were rejected. Reproducible results were obtained in subsequent studies under quasi-hydrostatic conditions with various internal pressure standards. They are compared

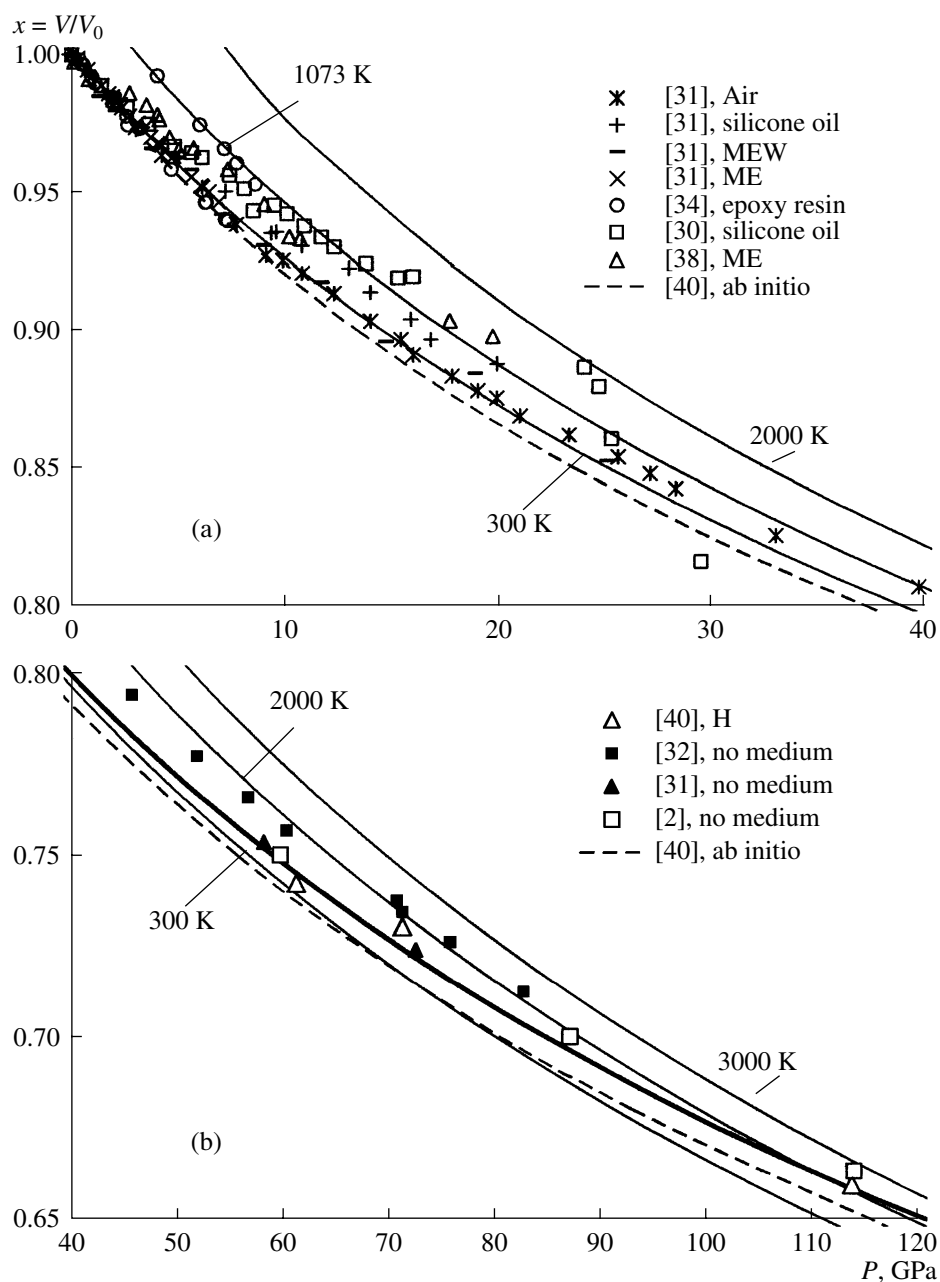


**Fig. 3.** Calculated isotherms and adiabat of magnesite compared with experimental data and first principles calculations [40]. (a) Isotherms of 300, 1073, and 2000 K at pressures of 0–40 GPa. (b) Isotherms of 300, 2000, and 3000 K and the shock-wave adiabat (thick line) at pressures of 40–120 GPa obtained in various pressure media, including Ar, epoxy resin, silicon oil, methanol–ethanol–water (MEW), and methanol–ethanol (ME), and under nonhydrostatic conditions (no medium). H denotes shock-wave data.

in Fig. 3 with the calculated isotherms of 300, 1073, 2000, and 3000 K and pressure values on the shock-wave adiabat. As can be inferred from this diagram, the use of silicon oil and methanol–ethanol–water as a pressure-transmitting medium does not provide hydrostatic conditions at pressures of above 12 GPa and 10 GPa, respectively. The results of measurements in an argon medium at pressures of higher than 20 GPa [31] revealed a certain influence of stress, which resulted in a significant pressure shift to higher values. The results

of  $P$ – $V$ – $T$  measurements by Zhang et al. [34], who used epoxy resin as a pressure medium, are in agreement with our calculations, including those for the 1073 K isotherm (Fig. 3a).

The  $P$ – $V$  and  $P$ – $V$ – $T$  relations of magnesite were also measured under nonhydrostatic conditions [2, 31, 32]. In order to minimize stresses, these authors used laser heating up to 2000–2500 K and quenching to room temperature under the same pressure at which

unit-cell parameters were measured; however, contradictory results were obtained (Fig. 3b). On the one hand, the room-temperature isotherms after [2, 31] appeared to be similar to the shock-wave adiabat and lie above our room isotherm. On the other hand, the room-temperature isotherms reported in [32] almost coincides with the calculated 2000 K isotherm. This discrepancy could be related either to different pressure scales used by these authors or to interlaboratory biases. Platinum was used as a pressure standard in [31, 32], whereas Isshiki et al. [2] obtaining the room-temperature isotherm on the basis of the ruby pressure scale for nonhydrostatic conditions [39]. The ruby scale significantly underestimates pressure at 50–100 GPa [13]. Taking into account this fact, the room-temperature isotherm of [2] must lie between the 2000 and 3000 K isotherms (Fig. 3b).

Thus, a comparison of calculations and experiments shows that the proposed equation of state of magnesite is consistent within the experimental errors with thermochemical, ultrasonic, X-ray, and shock-wave data and does not contradict first principles calculations [40]. The following values were obtained for the isothermal bulk modulus and its pressure derivative under standard conditions:  $K_T = 117.74$  GPa and  $K' = 4.06$ .

The values of  $K_T$  and  $K'$  reported in previous studies [29–36, 38] ranged from 99 to 156 GPa and from 2.3 to 9, respectively. It should be pointed out that the bulk moduli vary nonlinearly with temperature at atmospheric pressure (Fig. 2b), and they must be extrapolated to high temperatures with great care. As was noted above, simple equations of state linking  $P$ – $V$ – $T$  data only [34] provide an excellent approximation of volume as a function of temperature and pressure but do not permit an unequivocal choice of, say, isothermal bulk modulus (Fig. 2b).

Finally, let us constrain the stability field of magnesite using the thermodynamic data, i.e., calculate the equilibrium line of the reaction  $\text{MgCO}_3 = \text{MgO} + \text{CO}_2$ . Previous calculations [32] showed that, depending on the accepted slope  $(\partial K_T/\partial T)_P$ , magnesite can either be stable under the conditions of the Earth's lower mantle and outer core [if  $(\partial K/\partial T)_P = -0.021$  GPa/K] or decompose to periclase and carbon dioxide at a temperature of 3000 K and pressures of higher than 100 GPa [if  $(\partial K/\partial T)_P = -0.013$  GPa/K].

Since the numerical implementation of the proposed equation of state is rather complicated, Tables 2 and 3 list the Gibbs free energy of magnesite according to the

**Table 2.** Gibbs free energy of magnesite (kJ/mol) as a function of  $T$  and  $P$

Pressure, GPa	Temperature, K						
	298.15	500	1000	1500	2000	2500	3000
0	-1130.996	-1148.924	-1225.421	-1333.830	-1468.749	-1615.299	-1781.890
1	-1103.105	-1120.866	-1196.806	-1304.517	-1438.504	-1584.067	-1749.180
2	-1075.450	-1093.053	-1168.463	-1275.515	-1408.633	-1553.293	-1717.109
3	-1048.026	-1065.477	-1140.382	-1246.810	-1379.114	-1522.939	-1685.595
5	-993.830	-1010.999	-1084.959	-1190.228	-1321.040	-1463.367	-1624.004
10	-861.801	-878.351	-950.257	-1053.034	-1180.714	-1319.981	-1476.692
20	-610.140	-625.719	-694.397	-793.319	-916.308	-1051.106	-1202.394
30	-371.729	-386.557	-452.733	-548.695	-668.667	-799.667	-947.095
40	-143.952	-158.169	-222.297	-315.843	-432.543	-561.344	-705.740
50	74.959	61.258	-1.133	-92.632	-207.011	-333.540	-475.427
60	286.283	273.029	212.148	122.428	10.030	-114.510	-254.246
70	490.987	478.127	418.582	330.440	219.765	97.005	-40.844
80	689.830	677.321	618.975	532.251	423.097	301.957	165.792
90	883.419	871.228	813.969	728.535	620.739	501.092	366.450
100	1072.255	1060.353	1004.091	919.839	813.266	695.009	561.760
110	1256.866	1245.251	1189.733	1106.618	1001.154	884.201	752.235
120	1437.384	1425.933	1371.418	1289.223	1184.803	1069.081	938.305

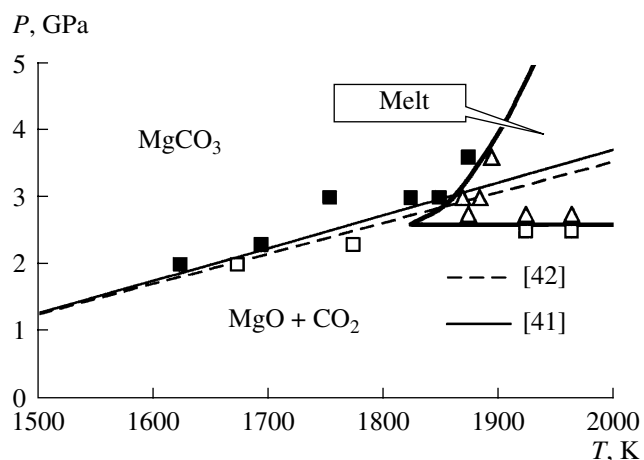


**Fig. 4.** Magnesite stability field after [43] compared with calculations for two different equations of state of  $\text{CO}_2$  [41, 42].

data of Table 1 and periclase [15] up to 3000 K and 130 GPa calculated as  $G_{T,P} = H_{T,P} - S_{T,P} \times T$ . The standard enthalpy was taken from [17], and the corresponding values of  $U_0$  (Eq. 1) are given in Table 1. The fugac-

ity of carbon dioxide was calculated using modern equations of state of  $\text{CO}_2$  [41, 42]. As expected, the calculated equilibrium line of the reaction  $\text{MgCO}_3 = \text{MgO} + \text{CO}_2$  is in good agreement with experimental data [43] in the region of high temperatures and relatively low pressures (Fig. 4). It was more interesting to calculate the equilibrium line of this reaction for the pressure–temperature region around 100 GPa and 3000 K, which is already accessible to experimental methods [2]. Our calculations with the equation of state of  $\text{CO}_2$  after [41] suggested that magnesite is stable at pressures of at least 130 GPa and 3000 K. The equation of state of  $\text{CO}_2$  after [42] is valid for pressures of up to 10 GPa, and  $\text{CO}_2$  fugacity at higher pressures was obtained by extrapolation (S. Churakov, personal communication). It appeared that the use of this equation of state of  $\text{CO}_2$  also indicated magnesite stability at pressures of at least 130 GPa and 3000 K. Thus, the calculations unambiguously demonstrated that magnesite is thermodynamically stable under the conditions of the Earth's lower mantle and outer core. It should be noted that this analysis ignored high-pressure structural transformations in magnesite, which were revealed by direct

**Table 3.** Gibbs free energy of periclase (kJ/mol) as a function of  $T$  and  $P$

Pressure, GPa	Temperature, K						
	298.15	500	1000	1500	2000	2500	3000
0	-609.686	-617.421	-650.920	-697.629	-753.394	-816.181	-884.819
1	-598.474	-606.131	-639.395	-685.835	-741.295	-803.732	-871.957
2	-587.328	-594.910	-627.949	-674.130	-729.299	-791.406	-859.249
3	-576.249	-583.758	-616.579	-662.512	-717.404	-779.198	-846.685
5	-554.280	-561.651	-594.057	-639.521	-693.893	-755.109	-821.945
10	-500.389	-507.449	-538.924	-583.344	-636.575	-696.547	-762.019
20	-396.451	-403.001	-432.940	-475.660	-527.072	-585.103	-648.510
30	-296.807	-302.947	-331.642	-372.998	-422.967	-479.489	-541.318
40	-200.743	-206.540	-234.187	-274.395	-323.162	-378.435	-438.972
50	-107.744	-113.248	-139.986	-179.201	-226.931	-281.133	-340.569
60	-17.424	-22.673	-48.608	-86.944	-133.760	-187.021	-245.491
70	70.519	65.497	40.282	2.735	-43.261	-95.679	-153.289
80	156.329	151.511	126.949	90.119	44.868	-6.787	-63.618
90	240.205	235.572	211.608	175.436	130.868	79.913	23.795
100	322.314	317.849	294.437	258.875	214.939	164.630	109.171
110	402.799	398.489	375.589	340.594	297.245	247.538	192.691
120	481.779	477.612	455.191	420.726	377.929	328.784	274.510

experimental measurements [2] and first principles calculations [3, 44] but could not be accounted for in our calculations because of the lack of thermodynamic data.

#### ACKNOWLEDGMENTS

The author thanks F.A. Letnikov (Institute of the Earth's Crust, Siberian Division, Russian Academy of Sciences) for his unfailing support of this research, A.R. Oganov (ETH, Zurich, Switzerland) as the first reviewer of the manuscript, and S.V. Churakov (PSI, Villigen, Switzerland) for the extrapolation of carbon dioxide fugacity into the region of ultrahigh pressures. This study was financially supported by the Russian Foundation for Basic Research, project nos. 05-05-64491 and 06-05-64579, and the Program for the Support of Leading Scientific Schools, project no. NSh-4496.2006.5.

#### REFERENCES

1. T. Katsura, Y. Tsuchida, E. Ito, et al., "Stability of Magnesite under the Lower Mantle Conditions," *Proc. Japan Acad. Ser. B, Phys. Biol. Sci.* **67**, 57–60 (1991).
2. M. Isshiki, T. Irifune, K. Hirose, et al., "Stability of Magnesite and Its High-Pressure Form in the Lowermost Mantle," *Nature* **427**, 60–64 (2004).
3. N. V. Skorodumova, A. B. Belonoshko, L. Huang, et al., "Stability of the MgCO<sub>3</sub> Structures under Lower Mantle Conditions," *Am. Mineral.* **90**, 1008–1011 (2005).
4. L. Liu, "Effects of CO<sub>2</sub> on the Phase Behavior of the Enstatite–Forsterite System at High Pressures and Temperatures," *Phys. Earth Planet. Inter.* **146**, 261–272 (2004).
5. O. L. Kuskov and N. I. Khitarov, *Thermodynamics and Geochemistry of the Core and Mantle of the Earth* (Nauka, Moscow, 1982) [in Russian].
6. Yu. I. Sidorov, "Mathematical Simulation of Complex Natural Systems," *Geokhimiya*, No. 1, 103–106 (2006) [*Geochem. Int.* **44**, 94–108 (2006)].
7. V. B. Polyakov and O. L. Kuskov, "Internally Consistent Model for the Calculation of Thermoelastic and Calorimetric Properties of Minerals," *Geokhimiya*, No. 7, 1096–1121 (1994).
8. T. V. Gerya, K. K. Podlesskii, L. L. Perchuk, et al., "Equation of State of Minerals for Thermodynamic Databases Used in Petrology," *Petrologiya* **6**, 563–578 (1998) [*Petrology* **6**, 511–526 (1998)].
9. T. V. Gerya, K. K. Podlessky, L. L. Perchuk, and W. V. Marresch, "Semi-Empirical Gibbs Free Energy Formulations for Minerals and Fluids for Use in Thermodynamic Databases of Petrological Interest," *Phys. Chem. Minerals* **31**, 429–455 (2004).
10. J. Hama and K. Suito, "Thermoelastic Models of Minerals and the Composition of the Earth's Lower Mantle," *Phys. Earth Planet. Inter.* **125**, 147–166 (2001).
11. L. Stixrude and C. Lithgow-Bertelloni, "Thermodynamics of Mantle Minerals—I. Physical Properties," *Geophys. J. Int.* **162**, 610–632 (2005).
12. P. I. Dorogokupets, "Critical Analysis of Equations of State for NaCl," *Geochem. Int.* **40**, S132–S144 (2002).
13. P. I. Dorogokupets and A. R. Oganov, "Equations of State of Cu and Ag and Revised Ruby Pressure Scale," *Dokl. Akad. Nauk* **391**, 515–518 (2003) [*Dokl. Earth Sci.* **391**, 854–857 (2003)].
14. P. I. Dorogokupets and A. R. Oganov, "Equations of State of Al, Au, Cu, Pt, Ta, and W and Revised Ruby Pressure Scale," *Dokl. Akad. Nauk* **410**, 239–243 (2006) [*Dokl. Earth Sci.* **410**, 1091–1095 (2006)].
15. P. I. Dorogokupets and A. R. Oganov, "Ruby, Metals, and MgO as Alternative Pressure Scales: A Semiempirical Description of Shock-Wave, Ultrasonic, X-Ray, and Thermochemical Data at High Temperatures and Pressures," *Phys. Rev. B* **75**, Art. No 024115 (2007).
16. S. V. Churakov, "Thermoelastic Properties of Solid Phases: C++ Object Oriented Library 'SolidEOS'," *Comp. Geosci.* **31**, 786–791 (2005).
17. T. J. B. Holland and R. Powell, "An Internally Consistent Thermodynamic Data Set for Phases of Petrological Interest," *J. Metamorph. Geol.* **16**, 309–343 (1998).
18. V. N. Zharkov and V. A. Kalinin, *Equations of State for Solids at High Pressures and Temperatures* (Nauka, Moscow, 1968; Consultants Bureau, New York, 1971).
19. P. Vinet, J. Ferrante, J. H. Rose, and J. R. Smith, "Compressibility of Solids," *J. Geophys. Res.* **92**, 9319–9325 (1987).
20. L. V. Al'tshuler, S. E. Brusnikin, and E. A. Kuz'menkov, "Isotherms and Gruneisen Functions for 25 Metals," *Prikl. Mekh. Tekh. Fiz.* **161**, 134–146 (1987).
21. A. R. Oganov and P. I. Dorogokupets, "Intrinsic Anharmonicity in Thermodynamics and Equations of State of Solids," *J. Phys. Condens. Matter.* **16**, 1351–1360 (2004).
22. P. I. Dorogokupets and A. R. Oganov, "Intrinsic Anharmonicity in Equations of State of Solids and Minerals," *Dokl. Akad. Nauk* **395**, 804–807 (2004) [*Dokl. Earth Sci.* **395**, 238–241 (2004)].
23. W. B. Holzapfel, "Effects of Intrinsic Anharmonicity in the Mie-Gruneisen Equation of State and Higher Order Corrections," *High Pressure Res.* **25**, 187–203 (2005).
24. B. S. Hemingway, R. A. Robie, J. R. Fisher, and W. H. Wilson, "Heat Capacities of Gibbsite, Al(OH)<sub>3</sub>, between 13 and 480 K and Magnesite, MgCO<sub>3</sub>, between 13 and 380 K and Their Standard Entropies at 298.15 K, and Heat Capacities of Calorimetry Conference Benzoic Acid between 12 and 316 K," *J. Res. U.S. Geol. Surv.* **5**, 797–806 (1977).
25. R. A. Robie, B. S. Hemingway, and J. R. Fisher, "Thermodynamic Properties of Minerals and Related Substances at 298.15 K and 1 Bar (10<sup>5</sup> Pascals) Pressures and at Higher Temperatures," *U.S. Geol. Surv. Bull.*, No. 1452 (1978).
26. S. A. Markgraf and R. J. Reeder, "High-Temperature Structure Refinements of Calcite and Magnesite," *Am. Mineral.* **70**, 590–600 (1985).
27. N. I. Christensen, "Elastic Properties of Polycrystalline Magnesium, Iron, and Manganese Carbonates to 10 Kilobars," *J. Geophys. Res.* **77**, 369–372 (1972).
28. P. Hubert and F. Plicque, "Proprietés élastiques de carbonates rhomboédriques monocristallins: calcite, magnesite, dolomite," *C. R. Acad. Sci. Paris* **275**, 391–304 (1972).

29. P. Gillet, "Stability of Magnesite ( $\text{MgCO}_3$ ) at Mantle Pressure and Temperature Conditions: A Raman Spectroscopic Study," *Am. Mineral.* **78**, 1328–1331 (1993).
30. G. Fiquet, F. Guyot, and J. P. Itie, "High-Pressure X-Ray Diffraction Study of Carbonates:  $\text{MgCO}_3$ ,  $\text{CaMg}(\text{CO}_3)_2$ , and  $\text{CaCO}_3$ ," *Am. Mineral.* **79**, 15–23 (1994).
31. G. Fiquet and B. Reynard, "High-Pressure Equation of State of Magnesite: New Data and a Reappraisal," *Am. Mineral.* **84**, 856–860 (1999).
32. G. Fiquet, F. Guyot, M. Kunz, et al., "Structural Refinements of Magnesite at Very High Pressure," *Am. Mineral.* **87**, 1261–1265 (2002).
33. N. L. Ross, "The Equation of State and High-Pressure Behavior of Magnesite," *Am. Mineral.* **82**, 682–688 (1997).
34. J. Zhang, I. Martinez, F. Guyot, and P. Gillet, "X-Ray Diffraction Study of Magnesite at High Pressure and High Temperature," *Phys. Chem. Minerals* **24**, 122–130 (1997).
35. N. G. Kalashnikov, M. N. Pavlovskii, G. V. Simakov, and R. F. Trunin, "Dynamic Compressibility of Calcite Group Minerals," *Izv. Akad. Nauk SSSR, Fiz. Zemli*, No. 2, 23–29 (1973).
36. J. Matas, O. Gillet, Y. Ricard, and I. Martinez, "Thermodynamic Properties of Carbonates at High Pressures from Vibrational Modeling," *Eur. J. Mineral.* **12**, 703–720 (2000).
37. L. V. Gurvich, I. V. Veits, V. A. Medvedev, et al., *Thermodynamic Properties of Individual Substances* (Nauka, Moscow, 1978–1982), Vols. 1–4 [in Russian].
38. S. A. T. Redfern, B. J. Wood, and C. M. B. Henderson, "Static Compressibility of Magnesite to 20 GPa: Implications for  $\text{MgCO}_3$  in the Lower Mantle," *Geophys. Res. Lett.* **20**, 2099–2120 (1993).
39. H. K. Mao, P. M. Bell, J. W. Shaner, and D. J. Steinberg, "Specific Volume Measurements of Cu, Mo, Pd, and Ag and Calibration of the Ruby R1 Fluorescence Pressure Gauge from 0.06 to 1 Mbar," *J. Appl. Phys.* **49**, 3276–3283 (1978).
40. L. Vocadlo, "First Principles Calculations on the High-Pressure Behavior of Magnesite," *Am. Mineral.* **84**, 1627–1631 (1999).
41. A. Belonoshko and S. K. Saxena, "A Molecular Dynamic Study of the Pressure–Volume–Temperature Properties of Supercritical Fluids:  $\text{CO}_2$ ,  $\text{CH}_4$ ,  $\text{CO}$ ,  $\text{O}_2$ , and  $\text{H}_2$ ," *Geochim. Cosmochim. Acta* **55**, 3191–3208 (1991).
42. S. V. Churakov and M. Gottschalk, "Perturbation Theory Based Equation of State for Polar Molecular Fluids: I. Pure Fluids," *Geochim. Cosmochim. Acta* **67**, 2397–2414 (2003).
43. A. J. Irving and P. J. Wyllie, "Melting Relationships in  $\text{CaO-CO}_2$  and  $\text{MgO-CO}_2$  to 36 Kilobars with Comments on  $\text{CO}_2$  in the Mantle," *Earth Planet. Sci. Lett.* **20**, 220–225 (1973).
44. A. R. Oganov, C. W. Glass, and S. Ono, "High-Pressure Phases of  $\text{CaCO}_3$ : Crystal Structure Prediction and Experiment," *Earth Planet. Sci. Lett.* **241**, 95–103 (2006).